

CHAPTER 5

MULTI LAYERED CABLE UNDER FREE BENDING - DEVELOPMENT OF NEW MATHEMATICAL MODEL AND VALIDATION

5.1 INTRODUCTION

This chapter extends the mechanical behaviour of bending response to a multi layered stranded cable under free bending. In-service conductors are always exposed to external loads: the axial tension is permanently exerted while transverse aeolian vibrations induce tension variations and a dynamic curvature along the span. When the conductor is subjected to external tension, an internal torque is induced which causes the conductor to unwind and as a result, any variation in tension excites a torsional vibration mode, transmitting a torque to the support. A theory has been developed to predict the static response of multi layered stranded cable subjected to free bending with combined effect of tension and torsion. Axially preloaded multilayered strands undergo plane-section bending only for sufficiently small lateral deflection. The stiffness matrix has been developed for multilayered cable and the relations are presented for axial, torsional and flexural rigidities and for coupling parameters. Also the mathematical formulation gives the resultant global strand axial force, strand twisting moment and strand bending moment. Numerical comparison has been made with available literature supported by verification with FE analysis.

5.2 DEVELOPMENT OF THE GENERAL MATHEMATICAL MODEL

A multilayered strand is made up of ‘n’ successive layers of helical wires laid contra helically over the core and the layers as shown in Figure 5.1.

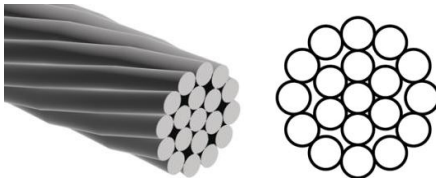


Figure 5.1 Multilayered cable assembly

The formulations presented in the previous chapters have been extended to the multilayered strands. An extension of the helical radius of the different layers is appropriately summed up using the Equation (5.1).

$$r_i = \left(R_c + 2 \sum_{j=1}^{i-1} R_j + R_i \right) \quad i = 1, 2, 3, \dots, n \quad (5.1)$$

5.2.1 Assumptions and Method of Approach

The present mathematical model in this chapter continues the same assumptions and method of approach of the previous chapter of single layered cable model. Additionally the model considered here is also analysed for the situation where a few of the outer wires are cut off.

5.2.2 Stiffness of the Stranded Cable

The Stranded cable global stiffness is derived using the stiffness matrix, relating the global strand loads to deformations and is same as equation (4.1) of chapter 4.

5.2.3 Wire Curvatures and Twist

The generalised curvatures and twist of a helical wire of any 'i'th layer subjected to a combination of axial deflection and bending of a strand are given by the Equations 5.2 to 5.4

$$\Delta\kappa = \frac{\sin \alpha_i (1 + \cos^2 \alpha_i) \sin \phi_i}{\rho} \quad (5.2)$$

$$\Delta\kappa' = \frac{-\sin^2 \alpha_i \cos^2 \alpha_i}{r_i} \varepsilon + \sin \alpha_i \cos \alpha_i (1 + \sin^2 \alpha_i) \frac{\delta\chi}{h} + \frac{\sin^4 \alpha_i \cos \phi_i}{\rho} \quad (5.3)$$

$$\Delta\tau = \frac{\sin \alpha_i \cos^3 \alpha_i}{r_i} \varepsilon + \sin^4 \alpha_i \frac{\delta\chi}{h} - \frac{\sin^3 \alpha_i \cos \alpha_i \cos \phi_i}{\rho} \quad (5.4)$$

5.2.4 Constitutive Equations

Similarly the constitutive equations derived for a helical wire of any 'i'th layer are given by the Equations 5.5 to 5.10

$$T_i = E_i A_i \sin^2 \alpha_i \varepsilon + E_i A_i r_i \sin \alpha_i \cos \alpha_i \frac{\delta\chi}{h} + \frac{E_i A_i r_i \sin^2 \alpha_i \cos \phi_i}{\rho} \quad (5.5)$$

$$G_i = \frac{E_i I_i \sin \alpha_i (1 + \cos^2 \alpha_i) \sin \phi_i}{\rho} \quad (5.6)$$

$$G_i' = \frac{-E_i I_i \sin^2 \alpha_i \cos^2 \alpha_i}{r_i} \varepsilon + E_i I_i \sin \alpha_i \cos \alpha_i (1 + \sin^2 \alpha_i) \frac{\delta\chi}{h} + \frac{E_i I_i \sin^4 \alpha_i \cos \phi_i}{\rho} \quad (5.7)$$

$$H_i = \frac{C_i J_i \sin \alpha_i \cos^3 \alpha_i}{r_i} \varepsilon + C_i J_i \sin^4 \alpha_i \frac{\delta \chi}{h} - \frac{C_i J_i \sin^3 \alpha_i \cos \alpha_i \cos \phi_i}{\rho} \quad (5.8)$$

$$N_i = -\frac{E_i I_i \sin^2 \alpha_i \cos \alpha_i (1 + \cos^2 \alpha_i) \sin \phi_i}{r_i \rho} \quad (5.9)$$

$$N'_i = \left(\frac{C_i J_i \sin \alpha_i \cos^5 \alpha_i}{r_i^2} + \frac{E_i I_i \sin^3 \alpha_i \cos^3 \alpha_i}{r_i^2} \right) \varepsilon + \left(\frac{C_i J_i \sin^4 \alpha_i \cos^2 \alpha_i}{r_i} - \frac{E_i I_i \sin^2 \alpha_i \cos^2 \alpha_i (1 + \sin^2 \alpha_i)}{r_i} \right) \frac{\delta \chi}{h} + \left(-\frac{C_i J_i \sin^3 \alpha_i \cos^3 \alpha_i \cos \phi_i}{r_i} - \frac{E_i I_i \sin^5 \alpha_i \cos \alpha_i \cos \phi_i}{r_i} \right) \frac{1}{\rho} \quad (5.10)$$

5.2.5 Equilibrium Equations of Stranded Cable

The total strand axial force, bending moment and twisting moment will be the summation of the forces and moments respectively from the core and the wires from the subsequent layers. The resultant external axial force, twisting moment and bending moment of the stranded cable have the wire components from Equations (5.5) to (5.10). All the forces on the core and the wires are projected along the axial direction of the strand and is given by the Equation 5.11

$$F_a = \sum_{i=1}^n m_i (T_i \sin \alpha_i + N'_i \cos \alpha_i) + E_c A_c \varepsilon \quad (5.11)$$

The total axial twisting moment acting on the central wire and the surrounding wires are given by the Equation 5.12

$$M_t = \left(\sum_{i=1}^n m_i \left[\begin{array}{l} H_i \sin \alpha_i + G'_i \cos \alpha_i + T_i r_i \cos \alpha_i \\ -N'_i r_i \sin \alpha_i \end{array} \right] \right) + C_c J_c \frac{\delta \chi}{h} \quad (5.12)$$

The bending moment of the stranded cable has been determined using Equation 5.13

$$M_b = \left(\sum_{i=1}^n m_i \begin{bmatrix} (T_i \sin \alpha_i + N'_i \cos \alpha_i) r_i \cos \phi_i \\ -H_i \cos \alpha_i \cos \phi_i + G_i \sin \phi_i \\ + G'_i \sin \alpha_i \cos \phi_i - N_i r_i \frac{\cos \alpha_i}{\sin \alpha_i} \sin \phi_i \end{bmatrix} \right) + \frac{E_c I_c}{\rho} \quad (5.13)$$

5.3 DEVELOPMENT OF THE FINITE ELEMENT MODEL

The finite element model for the multilayered cable was developed using a commercial CAE tool. Three dimensional solid brick elements have been used for structural discretisation. It may be pointed out that the interaction between wires of adjacent layers is characterised by two distinct types of contacts. The wires in the first layer touch the core continuously along a helical line. In contrast, the wires in the first layer and second layer cross each other making intermittent contacts called ‘‘Trellis contact’’. The geometric configuration as mentioned in Table 1 is such that, all the wires do not touch the neighbouring wires of the same layer but only touches the wires of the neighbouring layers as they cross over. The available ‘Master – Slave node concept’ was used here for the loading and extraction of reaction forces and moments from the multilayer finite element model. The parameters of the cable constructed are mentioned in section below.

5.3.1 Parameters of the Cable

The geometrical data has been adopted from K. C. Cutler and R. H. Knapp (2010) to study the bending response. The numerical data of the strand considered is presented in Table 5.1.

Table 5.1 Geometrical parameters and mechanical properties of 1x19 wire strand

Parameters	Core Wire	Layer 2	Layer 3
Number of Wires in a Layer	1	6	12
Radius of Wire (mm)	1.3845	1.2575	1.2575
Helix Radius (mm)	N/A	2.642	5.157
Helix Angle (Degree)	N/A	74.048°	76.925°
Young's modulus (Gpa)	200	200	200

The finite element model of the cable assembly thus generated (undeformed state) is shown in Figure 5.2. Three dimensional solid brick elements of 54700 numbers have been used for structural discretisation with a total of 268352 nodes. This model has been arrived after the mesh validation process of increasing the pitch length and increasing the mesh density. This configuration has been traded off based on the computation time and the accuracy.

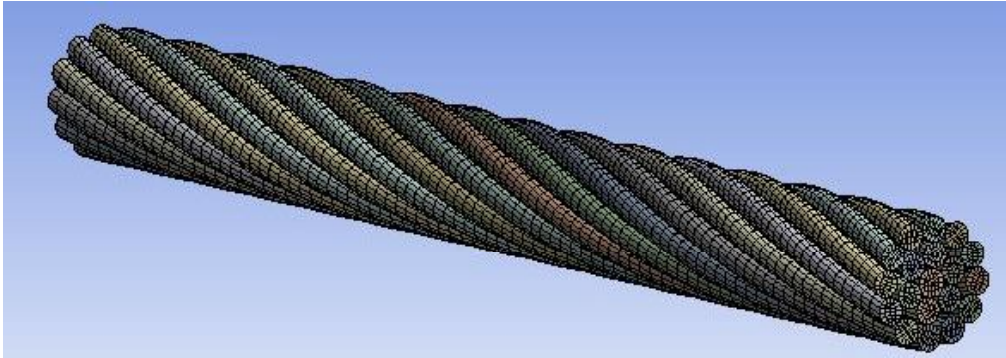


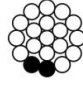
Figure 5.2 Multilayered finite element model of the cable assembly

The contact between the ‘core and wires of the first layer’ and ‘wires between the adjacent layers’ have been established as bonded contacts for the verification of the analytical model.

5.4 RESULTS AND DISCUSSIONS

The multilayered cable is numerically analysed for the parameter considered in Table 5.1. The combined effect of tension and torsion while it is subjected to free bending is explained in this section. The stiffness coefficients of the strand subjected to free bending was computed for the present model and the comparison of the same with Lantaigne (1985) model is presented in Table 5.2. Kee Jeung Hong (2005) published a paper on free bending on multilayered cable which is an extended version of the earlier model of Papailiou (1977). This work is however not considered here, as in their basic assumption itself, the torsional stiffness was considered to be negligible at the wire level.

Table 5.2 Stiffness coefficients of 1x19 wire strand

Stiffness coefficients	Lantaigne Model (1985)	Present Model	If 2 wires break off from the outer layer 	
			Lantaigne Model (1985)	Present Model
K_{aa} (N)	17522570	17524830	15686020	15688206
K_{at} (N-mm)	-9196165	-9204690	-6996529	-7007096
K_{ab} (N-mm)	--	--	8836645	8830001
K_{ta} (N-mm)	-9196165	-9204690	-6996529	-7007096
K_{tt} (N-mm ²)	19272969	25193106	16638467	21907084
K_{tb} (N-mm ²)	--	--	-10583647	-10765604
K_{ba} (N-mm)	--	--	8836645	8830001
K_{bt} (N-mm ²)	--	--	-10583647	-10765604
K_{bb} (N-mm ²)	172048910	172438699	146672104	129000257

Comparing the stiffness coefficients of the free bending case for both the models, the torsional rigidity coefficients showed a significant variation of 23% and the rest hardly less than 1%. This variation is attributed to the fact that Lanteigne (1985) omitted the wire twist and wire bending effect. The present model considers these effects together with wire stretch effects on the rotation of the wire. Among the additional components included in the present model, the wire twist dominated the rest. The stiffness coefficients K_{ab} , K_{ba} , K_{bt} , and K_{tb} are the coupling parameters that describe the static state of equilibrium with regard to bending. In the preslip scenario of a free bending case for both the models, the computation of these stiffness components, involves the summing up of the wire components for all angular positions and they tend to nullify with each other.

Also being curious, an analysis was extended to situations where two adjacent wires of the outermost layer have failed. In such cases the load is transferred to the adjacent wires and this leaves the conductor unbalanced thereby affecting the global response. The summing up of the wire components for all angular positions now do not tend to nullify with each other and thereby the stiffness coefficients of K_{ab} , K_{ba} , K_{bt} , and K_{tb} exist. Comparing the stiffness coefficients of the free bending cases subjected to two wires failure the coefficient of torsional rigidity of the present model showed a significant variation as high as 24% and the coefficient of flexural rigidity upto 13.6% lower.

The variation of bending moment for both the cases i.e normal situation and failure of neighboring wires were simulated using finite element models and the results of the same are presented in the Figure 5.3 and Figure 5.4.

The Figure 5.3 presents the comparison between the Lanteigne model, present analytical model, and present FEA model for two different

Poisson’s ratio ($\nu = 0.3$ and $\nu = 0.001$) for normal situation. Making a comparison of the analytical models alone, the present analytical model agreed well with Lanteigne model showed a variation of 0.23% on the higher side. This is attributed to the fact that the dominant wire twist factor does not significantly contribute to the bending moment of the cable.

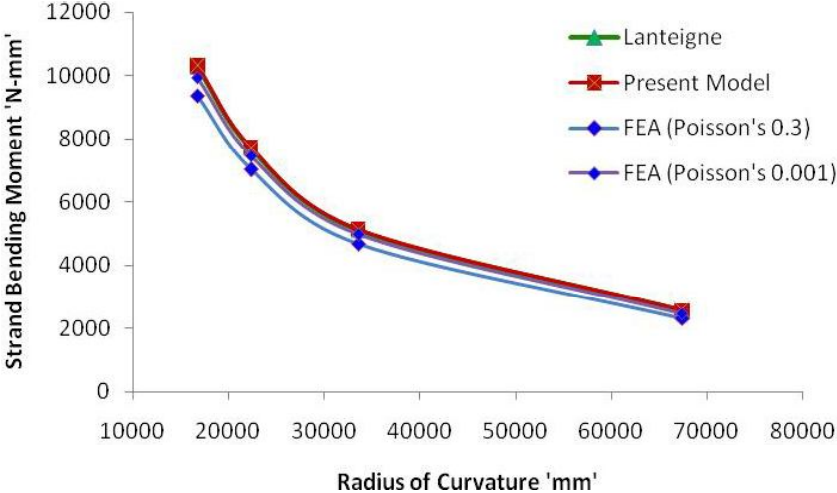


Figure 5.3 Variation of Bending Moment as a function of applied Radius of curvature

However, the bending moment computed from the finite element model with Poisson’s ratio of 0.001, predicted 3.6 % on the lower side for the given range of radius of curvature. With increase in the value of the Poisson’s ratio to 0.3 an increase in variation upto 10% was recorded.

In the second part of the study, i:e failure of two neighboring wires case, the bending moment computed for both analytical models and the finite element analysis are presented in Figure 5.4. Langtine (1985) model over predicted the bending moment value for the given range of radius of curvatures by 10 % with respect to the present analytical model. This is

attributed to the fact that Langtine (1985) has not considered the other wire component as mentioned above.

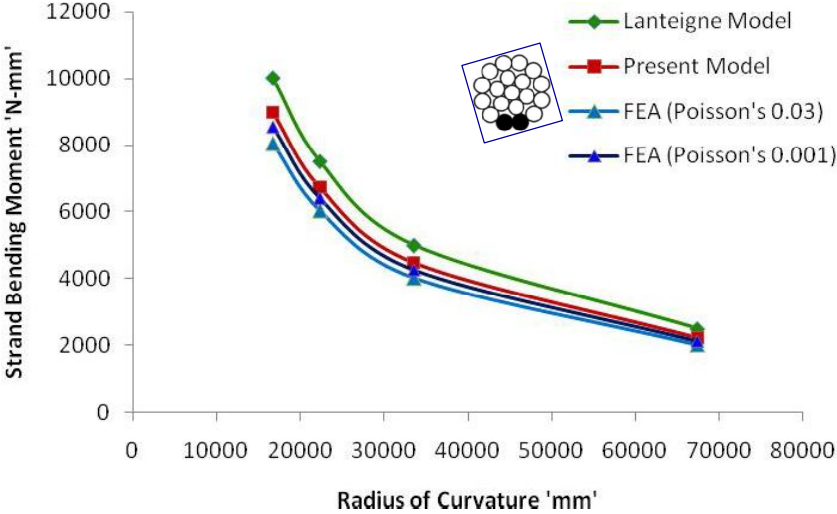
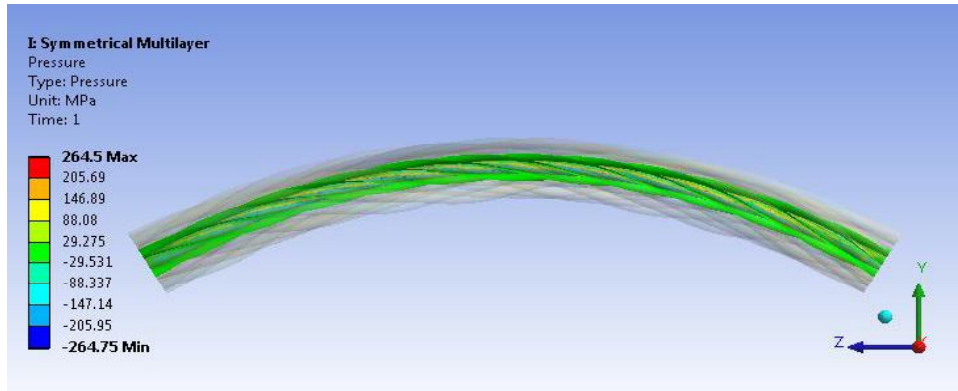


Figure 5.4 Variation of Bending Moment as a function of applied Radius of curvature for failure of two neighbouring wires of the outer layer

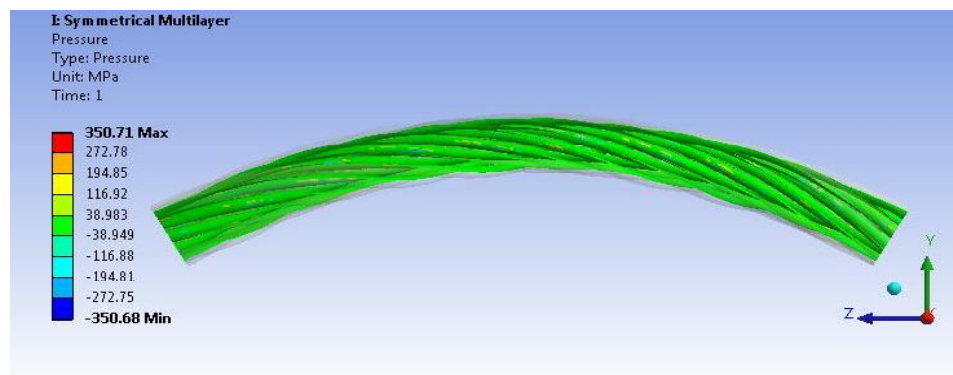
It is seen from Figure 5.4 that the present analytical model showed a variation of upto 4.7% and 10.5% on the higher side with the results of FE analysis for two different Poisson’s ratio ($\nu = 0.3$ and $\nu = 0.001$) respectively. It was observed that for the same range of variation of radii of curvature, the FE analysis with Poisson’s value of 0.3 under estimated the bending moments by 5.9% compared with that obtained using a Poisson’s ratio of 0.001.

The interaction between wires of adjacent layers is characterised by two distinct types of contacts. The wires in the first layer touch the core making a line contact which is continuous along a helical line. In contrast, the wires in the first layer and second layer cross each other making intermittent contacts called “Trellis contact”. The contact stress computed for these two

distinct types of contact for a radius of curvature 16 m is presented in Figure 5.5.



(a)



(b)

Figure 5.5 Contact stress for various applied radius of curvature:
(a) contact stress between the core and first layer of wires,
(b) contact stress between first layer and the second layer of wires

Likewise the contact stresses was also computed for the case with two wires broken on the outer layer. The comparative variation of the contact

stress for both the cases i.e, normal case and the case of two wires cut off is presented in Figure 5.6.

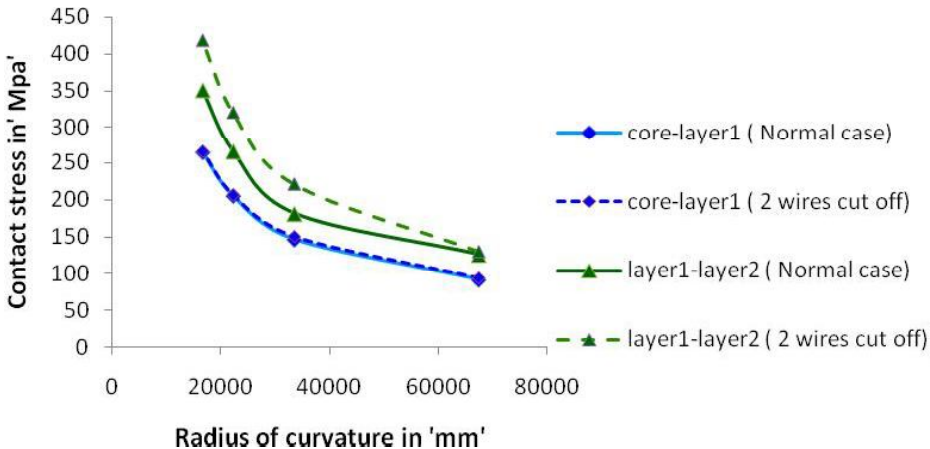


Figure 5.6 Contact stress between “core-layer 1” and “layer 1- layer 2” for various radius of curvature applied to normal case and 2 wire cut off case

It is observed that contact stresses developed at the contact helical line i.e the point of interaction between the core and wires of layer 1, maintains a fairly same magnitude of contact stress for both the cases. However, at instants where the interactions of wire happen between layer 1 and layer 2, it was noted that at large radii of curvature the magnitude of the contact stress were fairly same. With the decrease in the radius of curvature, the magnitude of contact stress for “2 wire cut case” noted a 16 % hike for the range of radii curvature examined.

Figure 5.7 presents the von-Mises stress distribution for the case of applied 16m of radius of curvature as input for both the cases namely, symmetrical and unsymmetrical case. The von-Mises stress for the ‘2 wire cut case’ as predicted reported a higher magnitude than that of the ‘normal case’. This is attributed due to the reduction in stiffness of the cable because of the two wires being cut off.

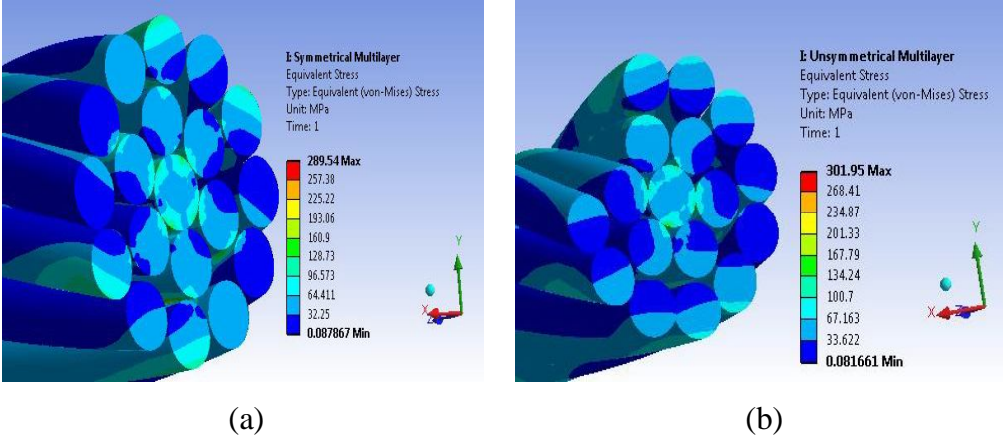


Figure 5.7 von Mises stress distribution recorded at the mid span of the cable length for: (a) normal case, (b) 2 wire cut off case

The study on failure of two neighboring wires case was carried out as failure of such wires on the strand will produce snaking of the cable between its extremities which is undesirable.

5.5 CONCLUSION

In this chapter a detailed analysis of mulilayered cable subjected to free bending has been presented. The stiffness matrix of the stranded cable subjected to tension, torsion and bending was arrived. Failure of two neighbouring wires in the outer layer of the cable was also additionally analysed to study the response of the coupling parameters, tension bending, and torsion bending.

A simulation for the multi layered cable assembly was individually conducted for two finite element models namely (i) the normal case and (ii) wire cutoff case. The responses of the cable for both the models were determined and where ever applicable the responses were related to the theoretical models of the present work and available literature.